Modelling and Simulation of Thermal Effect of Metastasis of Tumors in Human Limbs

Mamta Agrawal
Department of Mathematics
MANIT Bhopal, India

Neeru Adlakha
Department of Mathematics
SVNIT, Surat, India

K.R. Pardasani
Department of Mathematics
MANIT Bhopal, India

ABSTRACT
The present paper deals with the thermal effect model of temperature distribution in dermal layers of elliptical shaped human limbs involving two uniformly perfused tumor in dermis layer. Here the tumor is characterized by uncontrolled rates of metabolic heat generation. The normal tissues are characterized by self controlled metabolic heat generation. It is assumed that first there was only one tumor in the dermis but after sometime another tumor has developed at other position in the limb due to metastasis. The structure of the region has been taken into account by dividing the dermal region of the human limb into five layers. The outermost layer is the epidermis. Below the epidermis are the three layers of dermis followed by a layer of subermal tissues. The innermost solid cylinder is the limb core. Hexahedral elements have been used to discretize the whole region. Appropriate boundary conditions have been framed using the physical conditions. The seminumerical method has been used to obtain the temperature profiles.

Keywords
Heat transfer, Calculus of variations, Blood mass flow rate, Metabolic activity, Malignant tissues, Fourier series, Finite element method.

1. INTRODUCTION
In human body heat is generated every time. Even at complete rest or sleep or at the time of exercising heat is generated. Greater the exercise produce more and more heat. As a result body core temperature is also increases. But in order to maintain body core temperature 37^0C the Skin and Subcutaneous Tissue (SST) region plays an important role. It is boundary lamina, which consists of mainly two natural layers epidermis, and dermis. Below the skin there is an extensive network of blood vessels, lymphatic, fat cells and nerve fibers of subcutaneous tissue that rest upon body core. The heat transfers in blood vessels helps in maintaining uniform body core temperature irrespective of changes in environmental temperature. There are two more processes - metabolic heat generation (sum of physical and chemical changes), and sensible and insensible perspiration that help in maintaining uniform body core temperature. There are four avenues of heat loss: convection, conduction, radiation, and evaporation. If skin temperature is greater than that of the surroundings, the body can lose heat by radiation and conduction. But if the temperature of the surroundings is greater than that of the skin, the body actually gains heat by radiation and conduction. In such conditions, the only means by which the body can rid itself of heat is by evaporation. So when the surrounding temperature is higher than the skin temperature, anything that prevents adequate evaporation will cause the internal body temperature to rise. During sports activities, evaporation becomes the main avenue of heat loss. Humidity affects thermoregulation by limiting sweat evaporation and thus heat loss. A number of research workers have attempted to carry out experimental and theoretical investigations on temperature distribution problems in human body organs during the last few decades. Experimental investigations were carried out by Patterson [1] to determine the temperature profiles. The theoretical analysis and interpretation of the data in all the foregoing applications Chao [2,3], Cooper [4], Saxena [5,6], Sadakata [7] and Gurung [8] have been based on the widely used following bio heat equation given by Perl [9].

$$\rho c \frac{\partial T}{\partial t} = \mathrm{Div}.(K \,\mathrm{grad}\, T) + M(T_A - T) + S. \qquad (1)$$

Here, ρ, c, K, S and M are respectively the density, specific heat, thermal conductivity , rate of metabolic heat generation and blood mass flow rate in tissues. Further attempts have been made by Saxena and Pardasani [10], Pardasani and Adlakha [11] and Jain [12] to study problems involving abnormalities like tumors in SST regions of human body. Some models have been developed by Mitchell et.al [13], Pardasani and Adlakha [14, 15], Pardasani and Jas [16], Zhu et.al [17] and Song et. al [18] for temperature variation in human limbs for one and two dimensional steady cases under normal physiological and environmental conditions. Pardasani and Shakya [19] have extended finite element modeling to infinite domains. From the above literature survey, it is evident that all the research workers have assumed that human limb is perfectly circular in shape. But actually human limb is not perfect circular cylinder in shape, it may be considered as tapered elliptical cylinder in shape. So for realistic studies, it becomes necessary to develop a model to investigate temperature distribution considering elliptical shaped human limb involving metastasis of tumor. In view of this, Agrawal et.al have developed a model to study temperature variation in dermal layers of elliptical shaped human limbs by using Cubic Splines and Fourier Series approach [20]. Also they developed a two dimensional model to study thermal distribution in dermal regions involving metastasis tumors by using finite element method [21]. In this paper a semi numerical model a combination of Finite element method [22] and Fourier series [23] has been used.

2. MATHEMATICAL MODEL
The mathematical equation (1) for three-dimensional steady state case in elliptical coordinates may be written as:

$$\frac{1}{d^2(\sinh^2\mu+\sin^2\nu)}\left[K\frac{\partial}{\partial\mu}\left(\frac{\partial T}{\partial\mu}\right)+K\frac{\partial}{\partial\nu}\left(\frac{\partial T}{\partial\nu}\right)\right]+ K\frac{\partial}{\partial z}\left(\frac{\partial T}{\partial z}\right)+M(T_A-T)+S_1+W=0. \quad (2)$$

Here, S_1 and W respectively denote the self controlled and uncontrolled metabolic heat generation. Also μ, ν and z are elliptic-cylinder coordinates defined as follows:

$$x' = d\cosh\mu.\cos\nu,\ y' = d\sinh\mu.\sin\nu\ \ (0\le\nu\le 2\pi,\mu\ge 0),\ z' = z$$

Where, (x',y',z') are rectangular coordinates. The constant d is semi focal distance of elliptical shape which is defined as $d=\sqrt{(a')^2-(b')^2}$. Where a' and b' are the semimajor and semiminor axis of coaxial elliptical layers respectively. Also let d_i is the eccentricity of each layer which is given by $d_i = d/a'$. The outer surface of the limb is exposed to the environment and heat loss at this surface takes place due to conduction, convection, radiation and evaporation which is given as [5]:

$$-K\frac{\partial T}{\partial\mu}\Big|_{\mu=\mu_5} = h(T-T_a)+LE\,. \quad (3)$$

Where, h is the heat transfer coefficient, T_a is atmospheric temperature, L is Latent heat and E is rate of sweet evaporation. The blood moves in arteries from the trunk at body core temperature i.e. 37^0C into the limbs. This blood looses heat to the tissues while moving towards the extremities of the limbs. Thus the blood is at a lower temperature at extreme parts of the limbs. So the inner core temperature of the limb has been taken to be variable along the axial direction of the limb. Hence the following boundary conditions are imposed at the inner boundary [13]:

$$T(\mu_0,\nu,z)=G_{11}+G_{12}e^{-\xi z} \quad (4)$$

$$T_0(\nu,z)=T_{0a}(\nu)\ \text{at}\ z=a\ \text{and}\ T_0(\nu,z)=T_{0b}(\nu)\ \text{at}\ z=b \quad (5)$$

The two opposite sides of the inner core of the limb may be at different temperatures, so at the two ends of the limb the following parabolic variation of the core temperature along angular direction has been taken [21]

$$T_{0a}(\nu)=C_{1a}+C_{2a}\nu+C_{3a}\nu^2,\ T_{0b}(\nu)=C_{1b}+C_{2b}\nu+C_{3b}\nu^2 \quad (6)$$

Where,
$$T_{0a}(\nu)=T_{a0}\ \text{at}\ \nu=0$$
$$T_{0a}(\nu)=T_{a\pi}\ \text{at}\ \nu=\pi \quad (7)$$
$$T_{0a}(\nu)=T_{a0}\ \text{at}\ \nu=2\pi$$

and
$$T_{0b}(\nu)=T_{b0}\ \text{at}\ \nu=0$$
$$T_{0b}(\nu)=T_{b\pi}\ \text{at}\ \nu=\pi \quad (8)$$
$$T_{0b}(\nu)=T_{b0}\ \text{at}\ \nu=2\pi.$$

The temperature distribution in the limbs will be uniform along z-direction near the trunk, as the core temperature is uniform up to small distances from trunk. The other extremity of the limbs is assumed to be perfectly insulated and no heat loss takes place along the z-direction to the environment. Thus the flux along the z-direction at both the ends of the limbs is assumed to be zero as given below:

$$\frac{\partial T}{\partial z}=0\ \ \text{at}\ \ z=a\,,\ \frac{\partial T}{\partial z}=0\ \ \text{at}\ \ z=b \quad (9)$$

Since the radial distances are very small as compared to the axial distances, so the gradients at the two extremities of the limbs will be negligible. Also the thermoregulation process tries to preserve the heat by insulation and make up the heat loss by heat generation, thus reducing the temperature gradients to maintain the thermal balance. Now the dermal region of the limb is divided in to five concentric elliptic layers with different eccentricity d_1, d_2, d_3, d_4 and d_5. These layers have been further discretized into sub regions i.e. into 50 elements of elliptical sectors with two of its sides curved along angular direction. The angular points of each element are the nodes. Two uniformly perfused tumors in 18th and 48th element are assumed to be situated in the dermal region of the limb (see Fig. 1). The element information is summarized in Table-I.

The equation (2) and (3) are transformed into the following discretized variational form by using calculus of variations [22] for the e^{th} element:

$$I^{(e)}=\frac{1}{2}\iint_{\in 1}\left[K^{(e)}\{(\frac{\partial T^{(e)}}{\partial\mu})^2+(\frac{\partial T^{(e)}}{\partial\nu})^2+ A_1^{(e)}\left\{\begin{array}{l}\frac{\partial^2}{\partial z^2}(T^{(e)})^2+\\ M^{(e)}\left(T_A{}^{(e)}-T^{(e)}\right)^2\\ -2(S_1^{(e)}+W^{(e)})T^{(e)}\end{array}\right\}\right]d\mu d\nu \quad (10)$$
$$+\frac{\lambda^{(e)}}{2}\int_{\hat{I}2}A_1^{(e)}[h(T^{(e)}-T_a)^2+2L\,E\,T^{(e)}]d\nu\,.$$

Where, $A_1^{(e)}=d^{(e)2}(\sinh^2\mu^{(e)}+\sin^2\nu^{(e)})$ and e= 1, 2….50 .

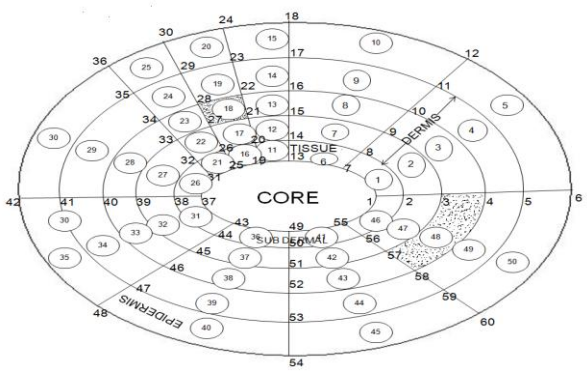

Figure 1 Finite element descretization of human limb

Table 1 Element information of Figure-1

e	i_e	j_e	k_e	l_e	e	i_e	j_e	k_e	l_e
1	1	2	7	8	26	31	32	37	38
2	2	3	8	9	27	32	33	38	39
3	3	4	9	10	28	33	34	39	40
4	4	5	10	11	29	34	35	40	41
5	5	6	11	12	30	35	36	41	42
6	7	8	13	14	31	37	38	43	44
7	8	9	14	15	32	38	39	44	45
8	9	10	15	16	33	39	40	45	46
9	10	11	16	17	34	40	41	46	47
10	11	12	17	18	35	41	42	47	48
11	13	14	19	20	36	43	44	49	50
12	14	15	20	21	37	44	45	50	51
13	15	16	21	22	38	45	46	51	52
14	16	17	22	23	39	46	47	52	53
15	17	18	23	24	40	47	48	53	54
16	19	20	25	26	41	49	50	55	56
17	20	21	26	27	42	50	51	56	57
18	21	22	27	28	43	51	52	57	58
19	22	23	28	29	44	52	53	58	59
20	23	24	29	30	45	53	54	59	60
21	25	26	31	32	46	55	56	1	2
22	26	27	32	33	47	56	57	2	3
23	27	28	33	34	48	57	58	3	4
24	28	29	34	35	49	58	59	4	5
25	29	30	35	36	50	59	60	5	6

In equation (10) $\lambda^{(e)}=1$ is only for those elements which are exposed to the environment and $\lambda^{(e)}=0$, for the remaining elements. Also $T_A^{(e)}$ is arterial temperature in each element has been taken equal to the core temperature of the limb.

$$T_A^{(e)}=T(\mu_0,\nu,z) \tag{11}$$

Here $W^{(e)}$ is assigned constant but different values in each layer. $W^{(e)}=0$ for normal tissues and $W^{(e)}>0$ for malignant tissues. In view of this $W^{(e)}$ is taken as $W^{(e)}=\eta^{(e)}s$, where s is the rate of metabolic heat generation in subdermal tissues, $\eta^{(e)}$ represents the ratio between the rates of metabolic activity in normal and malignant tissues. Here $\eta^{(e)}=0$ for normal tissues whereas $0\le\eta^{(e)}\le1$ denotes that rate of metabolic activity in malignant tissues is less than or equal to that in normal tissues. Also $\eta^{(e)}>1$ denotes that rate of metabolic activity in tumor is greater than that of normal tissues. Since the thickness of the layers is very small, the following linear variation with respect to position along radial direction is assigned to thermal conductivity, blood mass flow and metabolic heat generation in each layer:

$$K^{(e)}=\alpha_1^{(e)}+\alpha_2^{(e)}\mu,\ M^{(e)}=\beta_1^{(e)}+\beta_2^{(e)}\mu,\ S^{(e)}=\lambda_1^{(e)}+\lambda_2^{(e)}\mu$$

Where, $\alpha_1^{(e)},\alpha_2^{(e)}$, $\beta_1^{(e)},\beta_2^{(e)}$, $\lambda_1^{(e)}$ and $\lambda_2^{(e)}$ are given below [14]:

Subcutaneous tissues: e=1 (4) 46

$$\alpha_1^{(e)}=K_1,\ \alpha_2^{(e)}=0,\ \beta_1^{(e)}=M_1,\ \beta_2^{(e)}=0,$$
$$\gamma_1^{(e)}=S_1,\ \gamma_2^{(e)}=0,\ \lambda^{(e)}=0,\ W^{(e)}=0$$

Dermis : e=2+5i_1+5i_2, i_1 =0 (1) 9, i_2 =0 (1) 2.

Normal tissues:

$$\alpha_1^{(e)}=\frac{K_1\mu_2-K_3\mu_1}{\mu_2-\mu_1},\ \alpha_2^{(e)}=\frac{K_3-K_1}{\mu_2-\mu_1},\ \beta_1^{(e)}=\frac{M_1\mu_2-M_3\mu_1}{\mu_2-\mu_1}$$
$$\beta_2^{(e)}=\frac{M_3-M_1}{\mu_2-\mu_1},\ \gamma_1^{(e)}=\frac{S_1\mu_2-S_3\mu_1}{\mu_2-\mu_1}\ ,\ \gamma_2^{(e)}=\frac{S_3-S_1}{\mu_2-\mu_1}$$

Malignant tissues: (e=18, 48)

$$\alpha_1^{(e)}=K,\alpha_2^{(e)}=0,\ \beta_1^{(e)}=\tau^{(e)}m,\ \beta_2^{(e)}=0,\ \gamma_1^{(e)}=0,$$
$$\gamma_2^{(e)}=0,\ \lambda^{(e)}=0,W^{(e)}=\eta^{(e)}s$$

Here, $\tau^{(e)}$ and $\eta^{(e)}$ can be assigned any values depending on the type of tumors. As a particular case, it is assumed that the blood flow is almost the same in tumors and normal tissues. Thus $\tau^{(e)}=1$ for malignant tissues. Also two types of tumors have been considered, with metabolic rates respectively three and five times of that in normal tissues.

Epidermis: e=5 (4) 50

$$\alpha_1^{(e)}=K_3,\ \alpha_2^{(e)}=0,\ \beta_1^{(e)}=0,\ \beta_2^{(e)}=0,\ \gamma_1^{(e)}=0,$$
$$\gamma_2^{(e)}=0,\ \lambda^{(e)}=1,W^{(e)}=0$$

The following bilinear shape function for the variation of temperature within each element has been taken as:

$$T^{(e)}=\xi_1^{(e)}+\xi_2^{(e)}\mu+\xi_3^{(e)}\nu+\xi_4^{(e)}\mu\nu \tag{12}$$

Where, $\xi_1^{(e)},\xi_2^{(e)},\xi_3^{(e)}$ and $\xi_4^{(e)}$ are constants for the eth element. The eqs. (12) in matrix notation can be written as:

$$T^{(e)} = P^T \xi^{(e)} \tag{13}$$

Here, $P^T = [1 \ \mu \ \nu \ \mu\nu]$, $(\xi^{(e)})^T = [\xi_1^{(e)} \ \xi_2^{(e)} \ \xi_3^{(e)} \ \xi_4^{(e)}]$

Using nodal conditions we get,

$$T(\mu_\eta, \nu_\eta, z_\eta) = T_\eta ; \qquad \text{Where} \quad \eta = i,j,k,l \tag{14}$$

From equations (13) and (14) we get,

$$\bar{T}^{(e)} = P^{(e)} \xi^{(e)} \tag{15}$$

Where, $\bar{T}^{(e)} = \begin{bmatrix} T_i \\ T_j \\ T_k \\ T_l \end{bmatrix}$ and $P^{(e)} = \begin{bmatrix} 1 & \mu_i & \nu_i & \mu_i\nu_i \\ 1 & \mu_j & \nu_j & \mu_j\nu_j \\ 1 & \mu_k & \nu_k & \mu_k\nu_k \\ 1 & \mu_l & \nu_l & \mu_l\nu_l \end{bmatrix}$

From eq. (15) we have, $\xi^{(e)} = R^{(e)} \bar{T}^{(e)}$ (16)

where, $R^{(e)} = P^{(e)^{-1}}$ putting $\xi^{(e)}$ from eq. (16) in eq. (13) we get,

$$T^{(e)} = P^T R^{(e)} \bar{T}^{(e)} \tag{17}$$

The integral $I^{(e)}$ given in equation (10) can be put in the form

$$I^{(e)} = I_k{}^{(e)} + I_m{}^{(e)} - I_s{}^{(e)} + I_\lambda{}^{(e)} + I_\mu{}^{(e)} \tag{18}$$

Where, $I_k{}^{(e)} = \frac{1}{2} \int_{\nu i}^{\nu k} \int_{\mu i}^{\mu j} K^{(e)} \left[\left(\frac{\partial T^{(e)}}{\partial \mu} \right)^2 + \left(\frac{\partial T^{(e)}}{\partial \nu} \right)^2 \right] d\mu \, d\nu$ (19)

$$I_m{}^{(e)} = \frac{1}{2} \int_{\nu i}^{\nu k} \int_{\mu i}^{\mu j} A_1{}^{(e)} M^{(e)} \left[T_A{}^{(e)2} + T^{(e)2} \right] d\mu \, d\nu \tag{20}$$

$$I_{(s)}{}^{(e)} = \int_{\nu i}^{\nu k} \int_{\mu i}^{\mu j} A_1{}^{(e)} \left[M^{(e)} T_A{}^{(e)} + S_1{}^{(e)} + W^{(e)} \right] T^{(e)} \, d\mu \, d\nu \tag{21}$$

$$I_{(\lambda)}{}^{(e)} = \frac{\lambda^{(e)}}{2} \int_{\nu_j}^{\nu_l} A_1{}^{(e)} \left[h (T^{(e)} - T_a)^2 + 2 L E T^{(e)} \right] d\nu \Big|_{\mu=\mu_5} \tag{22}$$

$$I_\mu{}^{(e)} = \frac{1}{2} \int_{\mu_i}^{\mu_j} K^{(e)} A_1 \frac{\partial^2}{\partial z^2} (T^{(e)})^2 \, d\mu. \tag{23}$$

Now putting value of $T^{(e)}$ from (17) in (19), (20), (21), (22) and (23) and then minimizing with respect to each nodal point temperature with the assumption that the parameters $K^{(e)}, M^{(e)}$ and $S^{(e)}$ are constants but different in each layer, we get:

$$\frac{dI_k{}^{(e)}}{d\bar{T}^{(e)}} = \bar{A}^{(e)} \bar{T}^{(e)}, \quad \frac{dI_m{}^{(e)}}{d\bar{T}^{(e)}} = B^{(e)} \bar{T}^{(e)} \tag{24}$$

$$\frac{dI_s{}^{(e)}}{d\bar{T}^{(e)}} = G^{(e)} , \quad \frac{dI_\lambda{}^{(e)}}{d\bar{T}^{(e)}} = F^{(e)} \bar{T}^{(e)} + D^{(e)} \tag{25}$$

$$\frac{dI_\mu{}^{(e)}}{d\bar{T}^{(e)}} = H^{(e)} \frac{d^2 \bar{T}^{(e)}}{dz^2} \tag{26}$$

Where, $\bar{A}^{(e)} = R^{(e)T} \left[\bar{A}_{ij} \right]_{4x4} R^{(e)}$, $B^{(e)} = R^{(e)T} \left[B_{ij} \right]_{4x4} R^{(e)}$, $G^{(e)} = R^{(e)T} \left[G_i \right]_{4x1}$, $F^{(e)} = R^{(e)T} \left[F_{ij} \right]_{4x4} R^{(e)}$

$D^{(e)} = R^{(e)T} \left[D_i \right]_{4x1}$ and $H^{(e)} = R^{(e)T} \left[H_{ij} \right]_{4x4} R^{(e)}$

here, $\bar{A}_{ij}, B_{ij}, F_{ij}, H_{ij}$ $(i, j = 1,2,3,4)$ and G_i, D_i $(i = 1,2,3,4)$ are constants.

Now, from (18) we have following equation:

$$\frac{dI^{(e)}}{d\bar{T}^{(e)}} = \frac{dI_k{}^{(e)}}{d\bar{T}^{(e)}} + \frac{dI_m{}^{(e)}}{d\bar{T}^{(e)}} - \frac{dI_s{}^{(e)}}{d\bar{T}^{(e)}} + \frac{dI_\lambda{}^{(e)}}{d\bar{T}^{(e)}} + \frac{dI_\mu{}^{(e)}}{d\bar{T}^{(e)}} \tag{27}$$

On putting (24), (25) and (26) in (27) we get, a following set of differential equations in terms of nodal temperatures T_i.

$$\bar{X} \bar{T} - \bar{V} \frac{d^2 \bar{T}}{dz^2} = \bar{Y}. \tag{28}$$

Here,

$$\bar{X} = \sum_{e=1}^{N} \bar{M}^{(e)} \left[\bar{A}^{(e)} + H^{(e)} + F^{(e)} \right] \bar{M}^{(e)T}, \bar{T} = \left[T_1 \ T_2 \ \ldots\ldots T_N \right]^T$$

$$\bar{Y}^T = \sum_{e=1}^{N} \bar{M}^{(e)} \left[G^{(e)} - D^{(e)} \right], \quad \bar{V} = \sum_{e=1}^{N} \bar{M}^{(e)} B^{(e)} \bar{M}^{(e)T}$$

T_N denotes the N^{th} nodal temperature and N is the number of nodal points. Now, following Fourier series is applied to eliminate the variable z from the above equation (28):

$$T_0 = A_{00} + \sum_{n=1}^{\infty} A_{n0} \cos n\alpha z, \quad T_i = A_{0i} + \sum_{n=1}^{\infty} A_{ni} \cos n\alpha z \tag{29}$$

Where, $\alpha = \pi/b$ and the coefficients A_{00} and A_{n0} are known due to boundary condition (3). All coefficients A_{0i} and A_{ni} are obtained by solving the following system of linear equations obtained from (28), and (29).

$$X^{(1)} A_0 = p^{(1)}, \quad X^{(2)} A_n = p^{(2)} \tag{30}$$

Here, $X^{(v)}$ (v=1, 2) are square matrices of order (60 X 60). A_0 and A_n are column matrices of order (60 X 1) and they represent the matrices of coefficients A_{0i} and A_{ni} respectively. $p^{(\sigma)}$ $(\sigma=1,2)$ is column matrices of order (60 X 1). A computer program has been developed for the entire problem and temperature profiles are obtained in each subregion.

3. RESULTS AND DISCUSSION

In this section, numerical results are shown in the form of figures explaining the relationship observed between the physiological parameters. The parameters used [8, 14] are as follows:

K_1=0.06 cal/cm-min.deg.C, K_3=0.03cal/cm-min.deg.C,

L=579.0 cal/gm and h=0.009Cal/cm^2-min.deg.C

The results have been computed for the following case.

$T_a = 15^0C$, E=0, $T_b = 37^0C$, $T_\alpha = 34^0C$,

M_1=0.003 Cal/cm^3-min.deg.C, M_3=0, S_3=0,

S_1=0.0357 Cal/cm^3-min.deg.C, s=0.0357 Cal/cm^3-min.

k= 0.0845 Cal/cm-min.deg. C, m=0.003 Cal/cm^3-min.

The expression for nodal information is as given below:

Radial Coordinates: -

$\mu_i = a_{k-1}$ for i=k+6j : j=0(1)9 and k=1(1)6.

Here, constants a_i (i=0(1)5) can be assigned any value depending upon the sample of skin layers under study. Here as a particular case following values have been used [14].

a_0=6.0 cm, a_1=6.5 cm, a_2=6.65 cm, a_3=6.75 cm,

a_4=6.9 cm, a_5=7.1 cm.

Angular Coordinates:

$\nu_i = 0$ for i=1(1)6, $\nu_{i+6} = \nu_i + 45^0$ for i=1(1)12

$\nu_{i+6} = \nu_i + 15^0$ for i=13(1)30, $\nu_{i+6} = \nu_i + 45^0$ for i=31(1)54

Eccentricity:-

$d_i = d_{k-1}$ for i=k+6j : j=0(1)9 and k=1(1)6

The following set of eccentricities has been calculated. d_1=.0030 d_2=.0026 d_3=.0023 d_4=.0020 d_5=.0017

The graph in figure-2 and figure-3 is between temperature (T) and angle (ν) for η=3.0 and η=5.0. The continuous lines are for normal tissues while the broken lines are for malignant tissues.

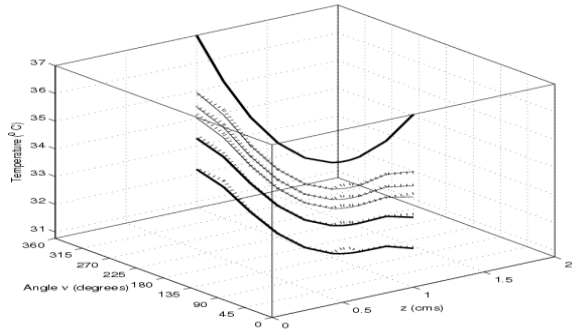

Figure 2 Graph between temperature (T) and angle (ν) at z=1 and η=3.0

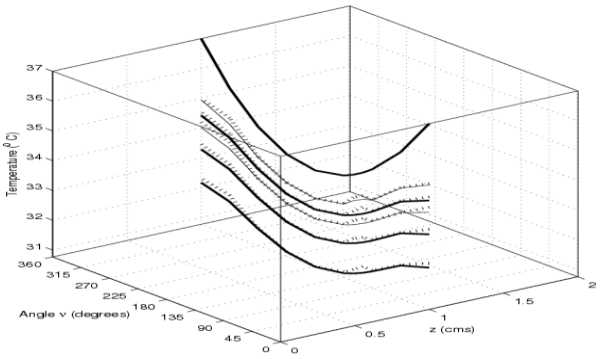

Figure 3 Graph between temperature (T) and angle (ν) at z=1 and η=5.0

The elevation in temperature profiles (broken lines) in each layer can be seen between $\nu=0^0$ to $\nu=45^0$, $\nu=90^0$ to $\nu=135^0$ and $\nu=315^0$ to $\nu=360^0$. The tumor is situated between $\nu=105^0$ to $\nu=120^0$ and also between $\nu=315^0$ to $\nu=360^0$. The maximum thermal disturbances are observed in these regions. The slope of the curves changes at $\nu=105^0$, 120^0 and $\nu=315^0$. Thermal disturbances are more between $\nu=315^0$ to $\nu=360^0$ and $\nu=0^0$ to $\nu=45^0$ as compared to $\nu=90^0$ to $\nu=135^0$. This is because the size of tumor is larger between $\nu=315^0$ to $\nu=360^0$ than that between $\nu=105^0$ and 120^0. The figure-4 and figure-5 represents the graph between Temperature T and radial distance μ at $\nu=105^0$ and 120^0 for η=3.0 and η=5.0 respectively. The elevation in temperature profiles (broken lines) is seen along radial direction towards the outer surface due to the presence of tumor in the dermis. This elevation is very small in the subdermal part but increases as we move towards the tumor in the dermis. The elevation in temperature profiles is more in the dermis and epidermis as compared to that in the subdermal part.

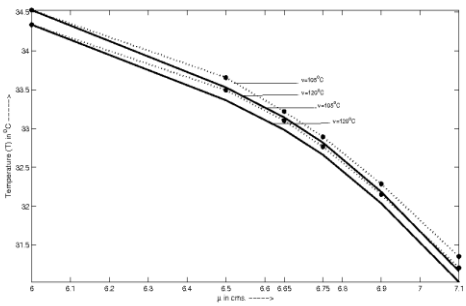

Figure 4 Graph between temperature (T) and radial distance (μ) at η=3.0

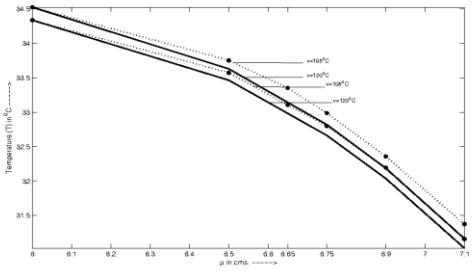

Figure 5 Graph between temperature (T) and radial distance (μ) at η=5.0

Further, from the above graphs it is observed that the thermal effect of tumor is more along radial direction as compared to that along angular direction. This is because the radial distances involved are small as compared to the angular distances. Also the temperature gradient is more along radial direction than that along angular directions. Thus heat flows more along the radial direction towards the outer surface in comparison to angular directions. The numerical results obtained here are quite similar and good agreement with the physiological facts as well as with those obtained by other researchers [10, 21]. The changes in the slope of the curves in the region of maximum thermal disturbances give us the idea about the position and size of the tumor. Here in figure-2 and figure-3 it is observed that elevation in temperature profiles is more for η=5.0 than for η=3.0. Thus the metabolic activity has significant thermal effects on the tumor. These results can be used to correlate the temperature profiles with the type of tumor.

From the above discussion, it is evident that thermal information of normal and malignant tissues can be useful for predicting the position, size and type of tumors. The seminumerical computational technique a combination of finite element method and Fourier series employed here has been quite successful in reducing the three dimensional problem further in to two-dimensional problem and obtaining useful results. The computations involved in this method are less as compared to those in variational finite element method [21]. This technique is also quite efficient and versatile as it has been possible to incorporate important variations of the parameters involved in the problem. Another important feature of this approach is that we have been able to incorporate the realistic geometric shape of the elliptical tapered shaped limb along three dimensions. This model can be further extended to incorporate more structural details of tumor.

4. ACKNOWLEDGMENTS

The authors are highly grateful to Department of Biotechnology, New Delhi, India for providing support in the form of Bioinformatics Infrastructure Facility for carrying out this work.

5. REFERENCES

[1] Patterson A.M., Measurement of temperature profiles in human skin, S.Afr.J.Sc. 1976; 72: 78-79.

[2] Chao K.N., Eisley J.G. and Yang W.J., Heat and water migration in regional skins and subcutaneous tissues, Bio.Mech. Symp, ASME,1973; 69-72.

[3] Chao K.N. and Yang W.J., Response of skin and tissue temperature in sauna and steam baths, Bio.Mech. Symp, ASME, 1975; 69-71.

[4] Cooper T.E., and Trezek G.J., A probe technique for determining the thermal conductivity of tissue J.Heat Trans., ASME, 94:1972; 133-140.

[5] Saxena V.P., Temperature distribution in human skin and subdermal tissues, J. Theo. Biol., 1983; 102: 277-286.

[6] Saxena V.P. and Gupta M.P., Steady state heat migration in radial and angular direction of human limbs, Ind. J. Pure. Appl. Math. 1991; 22 (8): 657-668.

[7] Sadakata Mieko and Yamada Yoshiaki, Perception of foot temperature in young women with cold constitution: Analysis of skin temperature and warm and cold sensation thresholds, J.Physiological Anthropology, 2007; 26: 449-457.

[8] Gurung D.B., Saxena V.P., P.R. Adhikary, Fem Approach to one dimensional unsteady state temperature distribution in human dermal parts with quadratic shape functions, J. Appl. Math. & Informatics Vol. 27 (2009), N0. 1-2, pp.301-313.

[9] Perl W., Heat and matter distribution in body tissues and determination of tissue blood flow by local clearance methods, J.Theo. Biol., 1962; 2: 202-235.

[10] Saxena V.P. and Pardasani K. R., Effect of dermal tumors on temperature distribution in skin with variable blood flow, Bull. Mathematical Biology, U.S.A., 1991; Vol.53: No.4: 525-536.

[11] Pardasani K.R. and Adlakha N., Exact solution to a heat flow problem in peripheral tissue layers with a solid tumor in dermis, Ind.J. Pure.Appl.Math, 1991; 22(8): 679-682.

[12] Jain R.K. Temperature distribution in normal and neoplastic tissues during Normothermia and hypothermia in ``Thermal characteristics of tumors: Application in detection and treatment '', R.K.Jain and Gullino, Nyas, 1980; Vol. 335: 48-62.

[13] Mitchell J.W., Galvez T. L, Hengle J., Myers G.E. and Siebercker K.L., Thermal response of human legs during cooling, J.Appl. Physiology, U.S.A., 1970; 29 (6): 859-865.

[14] Pardasani K.R. and Adlakha N., Two-dimensional steady state temperature distribution in annular tissue layers of a human or animal body, Ind.J.Pure and Appl. Math.,1993; 24(11): 721-728

[15] Pardasani K.R. and Adlakha N, Coaxial circular sector elements to study two- dimensional heat distribution problem in dermal

regions of human limbs. Mathl.Comput. Modeling, 1995; Vol.22, No.9: 127-140.

[16] Jas P., Finite element approach to the thermal study of malignancies in cylindrical human organs, Ph.D. Thesis, MANIT, Bhopa ; 2002.

[17] Zhu M., Weinbaum S. and Jiji L.M., Heat exchange between unequal counter current vessels asymmetrically embedded in a cylinder with surface convection, Int. J. Heat Mass Transfer,1990; Vol. No. 10: 2275-2284.

[18] Song W.J., Weinbaum S., Jiji L.M. and Lemons D., A combined macro and micro vascular model for whole limb heat transfer, Trans. ASME. J. Bio. Mechanical Engineering 1988; Vol. 110: 259-268.

[19] Pardasani K.R. and Shakya M., Infinite element thermal model for human dermal regions with tumors, Int. Journal of Applied Sc. & Computations, May 2008;Vol. 15, No. 1: pp. 1-10.

[20] Pardasani K.R., Agrawal M. and Adlakha N , Cubic Splines and Fourier Series Approach to Study Temperature Variation in Dermal Layers of Elliptical Shaped Human Limbs, International Journal of Computational and Mathematical Sciences 2; 4 © www.waset.org Fall (2008).

[21] Pardasani K.R., Agrawal M. and Adlakha N., Thermal disturbance in dermal regions of human limbs involving metastasis of tumors, International Mathematical Forum, 5, 2010, no. 39, 1903 - 1914,

[22] Rao S.S, The finite element method in engineering, Elsevier Science and Technology books: 2004.

[23] Saxena V.P. and Bindra J.S., Pseudo-analytic finite partition approach to temperature distribution problem in human limbs, Int. J. Math. Sciences. , 1989; Vol. 12: 403- 408.